Towards Efficient LEO-Constellation Design for Regional PNT Services

Elena Simona Lohan, *Senior Member, IEEE,* Kaan Çelikbilek, and Oana Cramariuc

Original scientific article

***Abstract*—The growing availability of low-cost positioning technologies enables broader access to advanced Positioning, Navigation, and Timing (PNT) services for regional and global applications. Building on our previous work, which introduced a Low Earth Orbit (LEO)–PNT optimization framework for Africa, we extend this framework to the European and Arctic region and demonstrate that well-designed regional constellations with only 65-85 satellites can match the performance of much larger LEO-PNT systems, such as those comprising 240-282 satellites. We evaluate both regional and global LEO-PNT performance in outdoor and indoor environments for several constellations: three newly designed configurations optimized for European coverage, a previously optimized African constellation, and seven benchmark constellations.**

***Index Terms*—Constellation Optimization, Coverage, Carrier-to-Noise Ratio, Dilution of Precision (DOP), Indoor-Outdoor Scenarios, LEO-PNT.**

I. Introduction

LOW Earth Orbit - Positioning, Navigation, and Timing (LEO-PNT) systems are increasingly seen as complementary layers to Global Navigation Satellite Systems (GNSS), forming part of a resilient, multi-orbit PNT ecosystem. Unlike GNSS, which are government-funded, LEO-PNT services are largely commercially driven, with companies such as Xona Space, Centispace, TrustPoint, and Iridium STL currently leading the way. Additionally, it is very likely that many of these LEO-PNT services will target regional coverage for applications such as autonomous driving, Arctic navigation, maritime navigation, urban mobility, or critical infrastructure timing [1], [2].

Ongoing European efforts on LEO-based PNT within the broader evolution of Europe's space infrastructure and capabilities have also been recently reviewed in [1]. An example is the development of a European in-orbit demonstrator for LEO-PNT, namely Celeste system [3], with the two "Pathfinder A" LEO-PNT satellites [4] scheduled for launch during early 2026. Such efforts show that research on LEO-PNT constellation optimization is timely as Europe advances towards integrating LEO constellations into its evolving space-based infrastructure.

This paper extends our previous work in [5] (which focused on African region for enhanced water-management and portable water-access applications) to LEO-PNT constellation optimization for European and parts of the Arctic region. The novelty of this paper comes from the main points below:

- Providing a clear and compact formulation of the LEO-PNT constellation design as a multi-optimization problem, by looking at six performance metrics (coverage, carrier-to-noise-ratio, geometric dilution of precision, drag, maintenance cost, and launch energy) in order to ensure a balanced assessment of system performance and feasibility.
- Proposing three new optimized small-size LEO-PNT constellations with maximum 85 satellites in the orbit for enhanced performance over European and Arctic regions;
- Inclusion of non-zero eccentricities in the optimization framework; this allows for better designs of low-sized constellations with very good PNT regional performance for users in European and Arctic region. We show that, with an eccentricity as a part of the optimization vector and with a focus on a region of interest instead of a global optimization, we can reach similar levels of performance in terms of coverage and dilution of precision metrics as constellations with three times more satellites.
- Presenting a detailed comparison in terms of PNT performance metrics between the three newly proposed constellations and eight other existing LEO-PNT constellations for both indoor and outdoor scenarios. Two carrier frequencies are considered in UHF and S-bands respectively, to cover the performance bounds under a wide frequency region. Moreover, these investigated frequency ranges match also with the European Space Agency proposals for future European LEO-PNT constellations [1]. The performance metrics included in our comprehensive comparisons are: the one-fold and four-fold coverages, the geometric and position dilution of precision, the carrier to noise ratios and the received powers, and the distributions of the number of visible satellites across regions.
- Offering design recommendations for optimized LEO-PNT constellations for Europe, with a focus on the expected trade-offs in stand-alone LEO-PNT design.

Manuscript received December 22, 2025; revised February 15, 2026. Date of publication March 25, 2026. Date of current version March 25, 2026. The associate editor prof. Roberto Garello has been coordinating the review of this manuscript and approved it for publication.

This paper was presented in part at the International Conference on Software, Telecommunications and Computer Networks (SoftCOM) 2025.

E. S. Lohan is with the Tampere Wireless Research Center, Tampere University, Finland (e-mail: elena-simona.lohan@tuni.fi). The work has been done when K. Çelikbilek was also with Tampere Wireless Research Center, Tampere University.

O. Cramariuc is with the Centrul IT pentru Stiinta si Tehnologie (CITST), Romania.

Digital Object Identifier (DOI): 10.24138/jcomss-2025-0291

II. METHODOLOGY

The methodology is comprised of three steps: an extended optimization-problem formulation based on our prior work in [5] and [6], a Non-dominated Sorting Genetic Algorithm III (NGSA-III)-based optimization, and comprehensive comparison between 11 constellations (three proposed here and eight benchmarks). We employ more clearly-defined optimization metrics and constraints than in our previous works [5], [6]. The NGSA-III-based optimization provides multiple solutions on the Pareto front of the multi-objective optimization problem. The comprehensive comparison between three selectively picked solutions from the Pareto front and eight other LEO-PNT constellations is done under multiple scenarios, not analysed in prior works, such as different frequency bands, different receiver sensitivities, and outdoor/indoor performance analysis.

A. Multi-objective Optimization Problem Formulation

Let us first define the constellation parameters to be optimized and the notations used in the optimization problem:

- N_{shells}, the number of orbital shells. A shell is defined as a unique combination of satellite altitudes, topology, and inclinations (h, T_p, i), allowing designs with different characteristics. This optimization parameter was only used in [6] and bounded to maximum 3 shells due to complexity reasons. In [5] and in this paper, as we focus on small-sized constellations with less than 102 satellites on orbit, we have set $N_{shells} = 1$.
- T_p: the orbital topology of each shell, chosen among two options, Walker Star and Walker Delta [6];
- i: the orbital inclination;
- N_{sv}: the total number of satellites in the constellation, distributed over N_{shells};
- n_p: the total number of orbital planes, distributed over N_{shells}
- h: the orbital altitude as a scalar or vector with N_{shell} elements, depending on N_{shell} value;
- e: the orbital eccentricity. In our previous works [5], [6] we assumed $e = 0$. However, by relaxing the assumption on e and looking also for non-zero values, one can enhance regional PNT performance, because in an elliptical orbit, the satellite slows down near the apogee, remaining longer over a particular region, which can be selected, e.g., as Europe or the Arctic as in this work. Thus, non-zero eccentricities hold the potential to provide prolonged visibility over target regions.

Let us introduce also the following notations:

- $\mathbf{x}$: the vector of the constellation parameters, which represents our unknown vector for a single-shell configuration: $\mathbf{x} = [N_{sv}, n_p, h, i, T_p, e]$.
- $\mathbf{p}_u$: the user 3D position, as a vector of three elements in x, y, and z directions;
- $\mathbf{E}_{\mathbf{p}_u}(\cdot)$: the expectation operator with respect to all considered users' positions $\mathbf{p}_u$;
- P_R: the receiver sensitivity, measured in dBm. Typical values of P_R, by analogy with GNSS, are between -155 dBm (for high-sensitivity receivers) and -127 dBm (for low-sensitivity receivers). In our work we considered both boundary values (-155 dBm and -127 dBm) in the performance analysis, but we solved the optimization problem under the assumption of a high-sensitivity receiver ($P_R = -155$ dBm) in order to investigate which is the lowest possible number of satellites of feasible constellations according to our optimization problem);
- α: the minimum elevation mask, meaning the elevation angle below which a satellite is considered as invisible on sky; during the optimization step, in order to capture strong-enough signals, we set $\alpha = 15^o$, but the performance analysis was done with $\alpha = 5^o$, which is a value chosen based on the reasoning that LEO satellites are expected to operate with elevation masks slightly smaller than those used with GNSS satellites, due to LEO closer proximity to Earth, and GNSS typical elevation masks are $7^o - 10^o$ [7], [8]).
- $\mathcal{C}_{4f}(\mathbf{x}, \mathbf{p}_u)$: the four-fold coverage defined as the percentage of user points 'seeing' at least four satellites at any given moment. The four-fold coverage depends primarily on the user position $\mathbf{p}_u$ and on the constellation parameters represented by $\mathbf{x}$, but also on the receiver sensitivity P_R as well as on the minimum elevation mask α because the visibility of the satellites depends on these two parameters. For example, more satellites are visible by receivers with low P_R and less satellites are visible is we increase α value. For clarity and compactness reasons, we dropped the P_R and α arguments from $\mathcal{C}_{4f}(\cdot)$, but we will mention their values in our results section.
- $\mathcal{C}_{1f}(\mathbf{x}, \mathbf{p}_u)$: the one-fold coverage defined as the percentage of user points 'seeing' at least one satellite at any given moment. While $\mathcal{C}_{1f}(\cdot)$: is not a metric in our multi-objective optimization problem, because $\mathcal{C}_{1f}(\cdot)$ and $\mathcal{C}_{4f}(\cdot)$ are highly correlated, we are considering also this metric in the performance analysis. For typical one-shot positioning algorithms, at least four satellites are needed in order to be able to estimate the 3D user position and the clock difference between the user and the satellites. However, 2D positioning can also be done based on a single satellite, observed at multiple times. This was done, for example, for Transit system [9], [10]; therefore $\mathcal{C}_{1f}(\cdot)$ is also a relevant performance metric to look at.
- $C/N_0(\cdot)$: the averaged received Carrier-to-Noise ratio in dB-Hz. This is an average over all visible satellites at a user location. In our implementation, we computed C/N_0 under the assumptions of wireless propagation channels based on Quadriga channel models [11], [12] and also assumed rain and fog absorption losses according to the ITU-R P.679-3 models [13]; C/N_0 depends both on the constellation parameters $\mathbf{x}$ and on the user position $\mathbf{p}_u$, as well as on the P_R and α assumptions.
- $GDOP$: the Geometric Dilution of Precision, which is a well-known satellite metric measuring the 'goodness' of the geometry of the visible satellites; a smaller value denotes a better geometry with respect to a considered user location $\mathbf{p}_u$; we used the weighted GDOP definition, in order to account for satellite-specific errors (ionospheric, tropospheric, clock, orbit, multipath, and tracking errors);

- $F_{\text{Drag}}(\cdot)$: is the satellite drag force, proportional to its relative speed and cross-sectional area, and is inversely related to altitude h. Therefore, F_{Drag} is a function of the constellation parameter vector $\mathbf{x}$; detailed formulation can be found in [6]. Note that F_{Drag} is independent on the user location, it only depends on the satellite location in orbit.
- $K(\mathbf{x})$: is the satellite launch cost and it is a metric proportional to the number of satellites in the constellation multiplied with the satellite's altitudes, as computed in [14] ($K((\mathbf{x}) = k_m N_{sv} h$, with k_m a constant depending on the satellite mass);
- $L_E(\mathbf{x})$ is the satellite launch energy, measured as the sum of the kinetic and gravitational potential energies required to launch a satellite to its orbit. It is a metric proportional to the orbital altitude h according to [15], namely $L_E(\mathbf{x}) = -\frac{k_{LE}}{2h}$, with k_{LE} another constant, also depending on the satellite mass, as well as on the gravitational constant); again, for the sake of the mathematical formulation, $L_E(\cdot)$ is parametrized as a function of the unknown vector $\mathbf{x}$, but in practice it only depends on one parameter of this vector, the orbital altitude.

With our parameters and notation explained, we formulate our multi-objective optimization problem as follows:

$$\mathbf{x}_{opt} = \underset{\mathbf{x}\in\mathcal{S}_\mathbf{x}}{min}\Big\{\mathcal{F}(\mathbf{x})\Big\} \tag{1}$$

where $\mathbf{x}_{opt}$ is the Pareto-optimal solution, $\mathbf{x}$ is the vector of constellation parameters to be optimized, $\mathcal{S}_\mathbf{x}$ is the set of all possible values of $\mathbf{x}$ and $\mathcal{F}(\cdot)$ is the multi-objective optimization vector whose individual elements must be minimized simultaneously. It is to be noted that the minus signs point out to metrics that actually need to be maximized:

$$\mathcal{F}(\mathbf{x}) = \begin{bmatrix} -\mathbf{E}_{\mathbf{p}_u}(\mathcal{C}_{4f}(\mathbf{x},\mathbf{p}_u)) \\ -\mathbf{E}_{\mathbf{p}_u}(C/N_0(\mathbf{x},\mathbf{p}_u)) \\ \mathbf{E}_{\mathbf{p}_u}(GDOP(\mathbf{x},\mathbf{p}_u)) \\ F_{Drag}(\mathbf{x}) \\ K(\mathbf{x}) \\ L_E(\mathbf{x}) \end{bmatrix} \tag{2}$$

It is to be remarked that the optimization metrics $\mathcal{F}(\mathbf{x})$ are independent on the individual $\mathbf{p}_u$, as we perform a statistical average over all considered user positions for the metrics in eq. (2), depending on user locations. Moreover, the multi-objective optimization problem defined in eq. (1) is done according to the following constraints:

$$\begin{aligned} h &\in [400:2000](km) \\ \mathbf{p}_u &\in \text{Desired grid (see Fig. 1)} \\ N_{sv} &\in [50:105] \\ n_p &\in [2:7] \\ i &\in [30^\circ:90^\circ] \\ T_p &\in \{W_{star}, W_{delta}\} \\ N_{sv} &= kn_p, \quad k \in \mathbb{N} \\ e &\in (0:0.1) \end{aligned} \tag{3}$$

The constraints from eq. (3) were chosen as follows: first, by focusing entirely on LEO orbits, i.e., altitudes h between 400 and 2000 km; secondly, by using an user grid of interest, as shown in Fig. 1: two regional ones (one region over Europe and Arctic circle and one region over Africa) and one global one (over the whole world, excluding the polar regions); thirdly, by aiming at low-sized constellations with maximum 105 satellites (the lower bound of 50 was set to speed up the convergence time because we noticed it was unlikely to get any feasible constellation with $N_{sv} < 50$).

The rest of the constraints used in eq. (3) were based on the following reasons: i) the orbital inclination cannot be higher than 90^o and, if we aim for European or Nordic latitudes, higher inclinations are necessary, therefore the lower inclination limit was set to an arbitrary and sufficiently low bound of 30^o, ii) N_{sv} must be an integer multiple of the number of planes n_p for symmetry purposes, in order to have an equal number of satellites per plane, iii) T_p, namely the shell topology, can only take one of the two values which are the most widespread in GNSS and LEO constellations: Walker Star (W_{star}) or Walker Delta (W_{delta}, and iv) we set an upper bound for the orbital eccentricity to 0.1 because $e > 0.1$ starts to create too large orbital altitude variations which would create highly uneven footprints and therefore, inconsistent satellite visibility; also optimization results have converged to very low e, between 0.0306 and 0.0446, thus the chosen upper bound is not restrictive in any way.

In terms of main differences with our prior work in [5] and [6], we point out the following subtle but important aspects: by including explicitly the cost and launch energy into the multi-objective optimization function and by imposing a stricter upper bound constraint of maximum 105 satellites, we have focused on more feasible constellations, suitable for regional deployments. By adding the eccentricity parameter as a parameter to be optimized, the optimized constellations allow for slight variations in altitudes (e.g., from perigee to the apogee of the orbit) and therefore enables more diverse combination of satellite–user line-of-sight directions, increasing the visibility of the satellites. In addition, by imposing a constraint of $e < 0.1$, such small but non-zero eccentricity has negligible operational downsides in terms of Doppler and drag variations. However, it improves the dilution of precision and satellite visibility for low satellite counts (e.g., as low as 66 based on our results).

B. Pareto-front Solutions

In multi-objective optimization functions, as the one in eq. (2), there is no unique optimization solution, but a set of so-called 'Pareto-optimal' solutions, placed on a Pareto-front. A Pareto-front is a set of solutions that form a boundary in the solution space where one cannot improve one of the optimization metrics without significantly worsening another optimization metric.

We adopted the adaptive weighting algorithm (ADaW) proposed by Li and Yao [16] to dynamically adjust the weights during the evolutionary optimization process, addressing one of the main challenges in our previous constellation optimiza-

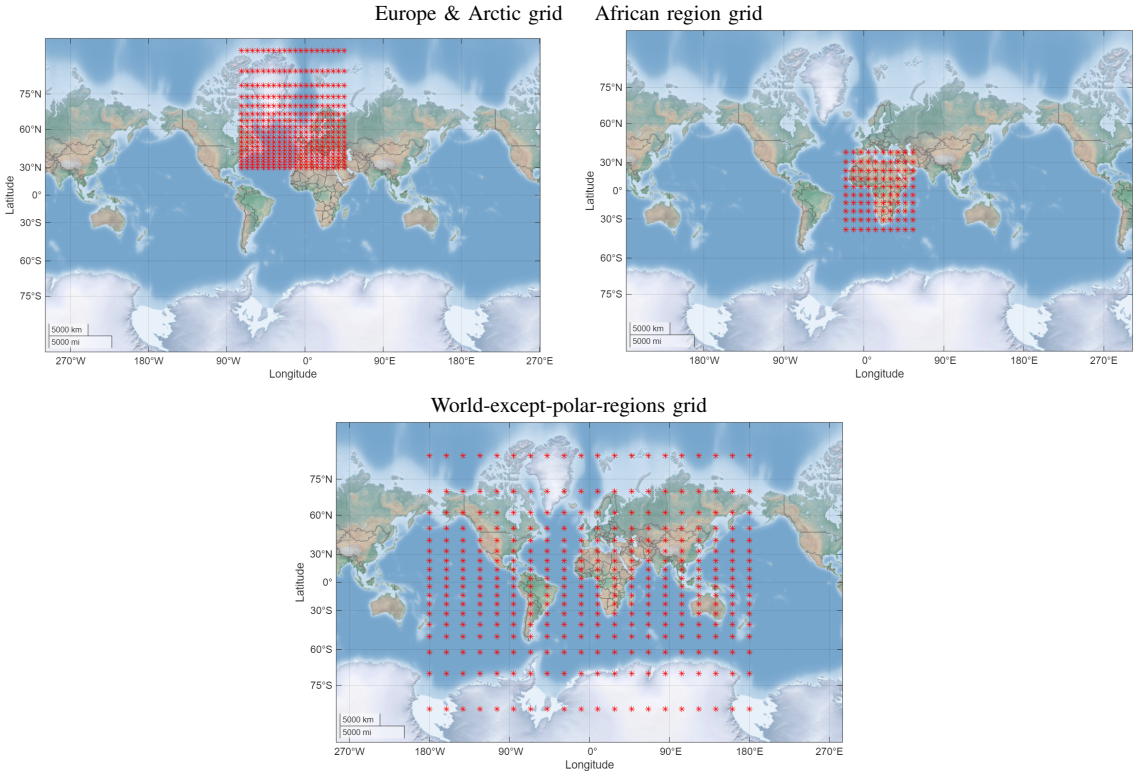

Fig. 1. User placement grids used in the simulations: $20 \times 20 = 400$ user points uniformly distributed over the region of interest. Upper plots: regional grids (Europe & Africa); lower plot: global grid.

tion studies. Evolutionary algorithms have shown strong performance for similar problems [17], making ADaW a natural fit. Unlike a classical multi-objective optimization problem, which would re-write $\mathcal{F}(\mathbf{x})$ from eq. (2) as a weighted sum of individual cost functions, with fixed weights, an AdaW approach adapts the weight vectors dynamically during the optimization process. By dynamically adjusting the weights, one can deal better with irregular Pareto-fronts or with non-convex cost functions. The AdaW algorithm generates, adds, deletes, and updates the weight vectors based on the geometry of the evolving population, seeking a set of weights that "fit" best to the Pareto-front, no matter on the Pareto-front shape.

To implement ADaW, we used the NSGA-III [6], [18], [19], designed for multi-objective optimization problems and selected also because it is compatible with ADaW and well-suited for irregular Pareto-fronts [19], which aligns with our six-objective constellation optimization problem. NSGA-III is a well-known and popular algorithm used for multi-objective optimization with several, typically higher than four, conflicting cost functions, such as minimizing launch energy, maximizing the coverage, etc. The NSGA-III works like an evolutionary algorithm [20], similar to the natural selection process, by following five steps: i) start with a population of randomly generated solutions within $\mathcal{S}_{\mathbf{x}}$ space; ii) evaluate each solution based on all the objectives from eq. (1); iii) use a non-dominated sorting to classify the solutions into layers (i.e., Pareto-fronts); iv) select the best individuals to survive and produce the next generation; v) use crossover and mutation to create new solutions. Instead of using crowding distance (as NSGA-II does), the NSGA-III uses reference points to maintain diversity. This ensures that no part of the Pareto front is ignored and one get well-distributed solutions. In general, NSGA-III works better than NSGA-II when we have at least four objectives in the multi-objective optimization problem. In our problem formulation we have six objectives, as shown in eq. (1).

For feasibility reasons of limiting the simulation durations, the Pareto-front is limited to 20 Pareto-optimal solutions in this work.

III. Proposed Constellations: Optimized for European Region

The Pareto-optimal solutions obtained from the multi-objective optimization problem from eqs. (1)-(3) are illustrated in the radar charts of Fig. 2. The upper plots in Fig. 2 show the normalized cost values of the Pareto-optimal solutions for the 6-metric cost vector from eq. (2), while the lower plots show the variations of the optimal parameters across the 20 Pareto-optimal solutions.

As seen in Fig. 2, most of solutions on the Pareto-front are quite close to each other. Thus, for further studies, for compactness reason, we down-selected three of them, on the basis of having three representatives as distinct as possible among the 20 Pareto-optimal solutions. The down-selected constellations are shown in red in the captions of the radar charts in Fig. 2. They were selected as follows: the one with the lowest number of orbital planes and lowest altitude (Pareto10 in the radar charts, renamed as OptEurope1 in Table

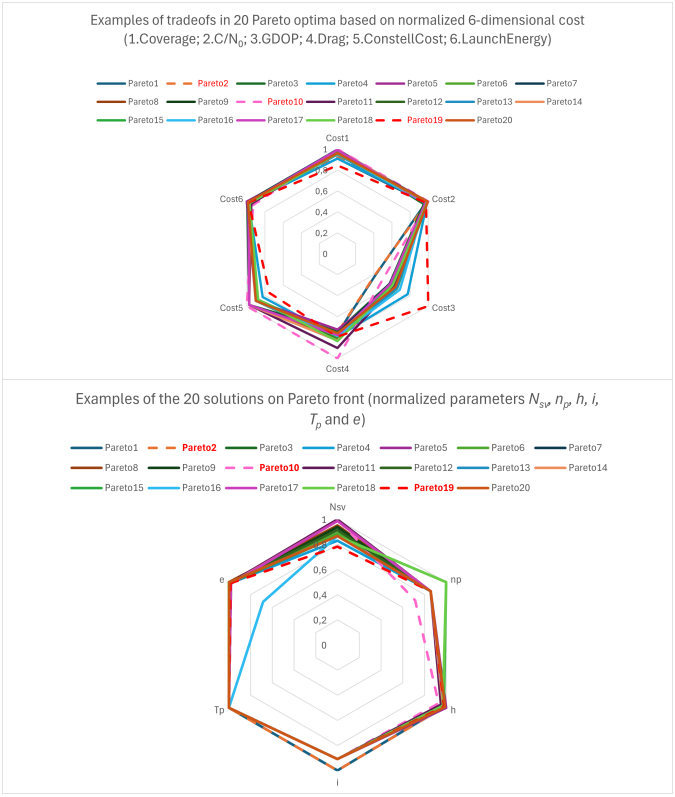

Fig. 2. Illustration of Pareto-optimal solutions in normalized radar charts. Upper plot: tradeoffs in terms of the 6-dimension normalized optimization metrics $\mathcal{F}_{norm}(\cdot) = [Cost1, \ldots, Cost6]^T$. Lower plot: tradeoffs in terms of $\mathbf{x}_{opt} = [N_{sv}, n_p, h, i, T_p, e]$. The solutions shown in red are down-selected for the comparisons with benchmarks in Section IV.

I), the one with the highest inclination (Pareto2 in the radar charts, renamed as OptEurope2 in Table I), and the one with the lowest number of satellites (Pareto19 in the radar charts, renamed as OptEurope3 in Table I). The full vector $\mathbf{x_{opt}}$ of the Pareto-optimal parameters of the new constellations are given in the last three rows (shown in green) in Table I. The rest of the rows in Table I show the eight other LEO-PNT constellations, selected as benchmarks. As many of those do not have their full parameters disclosed in the public domain, we used the notation '-like' for those with variable information available in open access and we added the references from where we took those parameters.

IV. Simulation-based Positioning Performance in Outdoor and Indoor Scenarios

The next methodological step has been to compare the 11 LEO-PNT constellations from Table I under two scenarios (one outdoor and one indoor) and under two carrier frequency assumptions (one in UHF band at 0.45 GHz carrier and another one in S-band at 2.4 GHz [1]). A 5 degree elevation mask was considered in these simulations and two P_T values were compared: $P_T = -155$ dBm and $P_T = -127$ dBm. The Effective Isotropic Radiated Power (EIPR) was adjusted to the carrier frequency for a fairer comparison, according to [27]:

$$EIRP = 54.1 - 20log_{10}\left(1.2 * 1e9 * (f_c)^{-1}\right) \quad (4)$$

where f_c is the carrier frequency in Hz. The indoor and outdoor channel models followed the Quadriga indoor and outdoor urban models [11]. We also included fog and rain attenuations according to the models in [13].

Table II shows an example of the comparative performance of 11 constellations over the Europe-plus-Arctic grid. Similar observations as the ones seen in Table II have also been drawn from the comparisons over Africa and World grids. However, due to lack of space, the results over the other world regions are only briefly shown in the Figs. 3 and 4 for outdoor and indoor scenarios, respectively. Different colours of the bars in Figs. 3 and 4 correspond to different world regions (light and dark magenta for Africa, light and dark orange for Europe and the Nordic region, and light and dark green for the whole world except the polar region, according to the grids depicted in Fig. 1). The dark colours are for the lower considered frequency (in UHF band, with better indoor penetration and lower path losses) and the light colours are for the upper considered frequency (in S-band). Moreover, boxplots comparisons among the three geographical grids (Europe, Africa, worlds) in are shown in Fig. 5 for GDOP, in Fig. 6 for C/N_0, and in Fig. 7 for the number of visible satellites.

The eight benchmark constellations are explained below and sorted alphabetically, as follows:

1) ESA-PNT/Celeste-like [3], [21]: ESA's Celeste mission is a compact LEO-PNT demonstration constellation now in development under ESA contracts. Some of the first papers mentioning it [21] were suggesting a dual-shell constellation on LEO and MEO orbits at 1200 and 8000 km, respectively. These are the altitudes we considered in our simulations, with the note that more recent works are suggesting significantly lower altitudes (e.g., around 510km [3]). This suggests that the results we present here for ESA-PNT constellation may be more optimistical than what can be achieved with lower-altitude constellations and can be considered as some performance upper bounds.
2) Iridium Next-like [22]: Iridium Next is not a dedicated LEO-PNT system. Iridium Next is primarily a global LEO satellite communications constellation designed for voice and data services, but it has been used many times as reference constellation in LEO-PNT studies because it is a low-sized constellation with global coverage and can illustrate the lower-bound performance metrics achievable with low-sized un-optimized constellations for positioning targets.
3) Centispace-like [23]: Centispace is a commercial LEO-based PNT augmentation system developed by Beijing Future Navigation Technology and one of the first commercially available LEO-PNT solutions. Its exact parameters varied in the open-access literature; the ones adopted in our paper followed the specifications in [23].
4) OptMarchionne [24]: The optimal Marchionne constellation was one of the three constellations proposed in [24], based on a constellation optimization approach over the the world grid (except the polar regions). The optimization approach in [24] differs from ours, e.g., different optimization problem formulation and different

TABLE I

PARAMETERS FOR THE TESTED CONSTELLATIONS (THREE PROPOSED ONES AND EIGHT BENCHMARK ONES); THE PROPOSED CONSTELLATIONS HAVE LESS THAN 85 SATELLITES (SMALL SIZES); FOR A FAIR COMPARISON, ALL BENCHMARK CONSTELLATIONS HAVE BELOW 300 SATELLITES (SMALL AND MEDIUM SIZES).

Constellation name*	Orbit type	Total N_{sv}	e	Topology** per shell	N_{shells}	N_{sv} per shell	Inclinations[^{o}] per shell	N_{planes} per shell	Altitudes [km] per shell	f_c [GHz]
ESA-PNT/Celeste-like [21]	LEO/ MEO	282	0	1/2	2	264/18	70/70	8/1	1200/8000	0.46, 2.4
Iridium Next-like [22]	LEO	66	0	1	1	66	86.4	6	780	0.46, 2.4
Centispace-like [23]	LEO	190	0	1/1/1	3	120/30/40	55/87.4/30	12/3/4	975/1100/1100	0.46, 2.4
OptMarchionne [24]	LEO	246	0	1/1/1	3	36/114/96	6/6/6	2/46/82	1250/1250/1250	0.46, 2.4
OptGlobal [6]	LEO	281	0	2/1/1	3	132/99/50	34/78/80	11/11/10	1790/1462/1286	0.46, 2.4
OptAfrica [5]	LEO	102	0	2	1	102	38	6	1442	0.46, 2.4
Xona-like [25]	LEO	258	0	1/1	2	198/60	53/97	18/6	1080/525	0.46, 2.4
SouthKoreaConstell [26]	LEO	240	0	2	1	240	55	8	1200	0.46, 2.4
OptEurope1 (proposed here)	LEO	85	0.0441	2	1	85	70	5	1826	0.46, 2.4
OptEurope2 (proposed here)	LEO	72	0.0443	2	1	72	77	6	1929	0.46, 2.4
OptEurope3 (proposed here)	LEO	66	0.0439	2	1	66	70	6	1924	0.46, 2.4

TABLE II

COMPARATIVE PERFORMANCE (AS AVERAGE VALUES OVER THE EUROPEAN PLUS ARCTIC GRID) OF THE 11 LEO-PNT CONSTELLATIONS PRESENTED IN TABLE I; THE LAST THREE CONSTELLATIONS ARE THE SMALL-SIZED PARETO-OPTIMAL ONES OVER THE EUROPEAN REGION.

Constellation	Scenario/f_c (GHz)	N_{sv}	Coverage (%)		GDOP [-]	PDOP [-]	EIRP [dBm]	Rx power [dBm]	$\mathbf{C/N_0}$ (dB-Hz)
			4-fold	1-fold					
ESA-PNT/Celeste-like	Outdoor / 0.46	282	100.000	100.000	1.874	1.718	36.854	-109.492	59.484
	Outdoor / 2.4		100.000	100.000	1.866	1.714	51.558	-109.550	59.426
	Indoor / 0.46		97.435	98.910	2.286	2.090	36.854	-142.711	26.264
	Indoor / 2.4		65.533	75.123	3.016	2.774	51.558	-147.631	21.344
Iridium Next-like	Outdoor / 0.46	66	54.452	98.481	5.159	4.724	36.854	-106.319	62.656
	Outdoor / 2.4		54.421	98.481	5.164	4.732	51.558	-106.418	62.557
	Indoor / 0.46		52.485	97.342	5.142	4.707	36.854	-139.164	29.811
	Indoor / 2.4		35.256	77.048	4.914	4.471	51.558	-145.576	23.399
Centispace-like	Outdoor / 0.46	190	98.435	100.000	4.420	4.097	36.854	-108.245	60.731
	Outdoor / 2.4		98.400	100.000	4.421	4.100	51.558	-108.325	60.650
	indoor / 0.46		95.567	99.729	4.548	4.209	36.854	-141.301	27.674
	Indoor / 2.4		62.819	88.117	5.075	4.679	51.558	-147.095	21.881
OptMarchionne	Outdoor / 0.46	246	81.883	85.000	3.201	2.950	36.854	-109.312	59.663
	Outdoor / 2.4		81.890	85.000	3.191	2.941	51.558	-109.387	59.588
	Indoor / 0.46		76.513	81.600	3.182	2.922	36.854	-142.336	26.639
	Indoor / 2.4		52.090	61.227	3.515	3.229	51.558	-147.827	21.148
OptGlobal	Outdoor / 0.46	281	100.000	100.000	2.429	2.217	36.854	-109.293	59.682
	Outdoor / 2.4		100.000	100.000	2.440	2.225	51.558	-109.391	59.584
	Indoor / 0.46		98.638	99.537	2.582	2.350	36.854	-142.551	26.424
	Indoor / 2.4		75.721	87.675	3.194	2.889	51.558	-147.839	21.136
OptAfrica	Outdoor / 0.46	102	48.000	61.952	5.190	4.783	36.854	-110.465	58.510
	Outdoor / 2.4		47.994	61.938	5.185	4.766	51.558	-110.530	58.445
	Indoor / 0.46		42.423	58.835	5.173	4.754	36.854	-144.091	24.885
	Indoor / 2.4		20.883	35.696	5.055	4.600	51.558	-148.571	20.404
Xona-like	Outdoor / 0.46	258	100.000	100.000	2.221	2.026	36.854	-110.456	58.520
	Outdoor / 2.4		100.000	100.000	2.230	2.034	51.558	-110.550	58.425
	Indoor / 0.46		99.560	99.954	2.459	2.237	36.854	-143.198	25.777
	Indoor / 2.4		83.235	93.715	3.521	3.179	51.558	-148.268	20.708
SouthKoreaConstell	Outdoor / 0.46	240	99.973	100.000	4.196	3.886	36.854	-107.642	61.333
	Outdoor / 2.4		99.967	100.000	4.164	3.857	51.558	-107.730	61.245
	Indoor / 0.46		97.952	99.898	4.433	4.096	36.854	-140.539	28.436
	Indoor / 2.4		71.146	92.777	5.049	4.662	51.558	-146.493	22.483
OptEurope1	Outdoor / 0.46	85	100.000	100.000	3.372	3.095	36.854	-112.051	56.924
	Outdoor / 2.4		100.000	100.000	3.353	3.077	51.558	-112.170	56.805
	Indoor / 0.46		88.721	93.881	3.598	3.287	36.854	-144.563	24.412
	Indoor / 2.4		48.179	61.806	3.924	3.567	51.558	-149.359	19.616
OptEurope2	Outdoor / 0.46	72	99.971	100.000	3.098	2.797	36.854	-112.195	56.781
	Outdoor / 2.4		99.971	100.000	3.100	2.798	51.558	-112.313	56.662
	Indoor / 0.46		85.881	94.402	3.324	2.990	36.854	-144.494	24.481
	Indoor / 2.4		41.244	57.392	4.993	4.560	51.558	-149.492	19.483
OptEurope3	Outdoor / 0.46	66	99.950	100.000	4.007	3.658	36.854	-112.413	56.562
	Outdoor / 2.4		99.946	100.000	3.993	3.644	51.558	-112.531	56.444
	Indoor / 0.46		86.023	94.283	4.426	4.030	36.854	-145.016	23.959
	Indoor / 2.4		41.244	57.391	4.993	4.560	51.558	-149.492	19.483

optimizer algorithm. However, the results in [24] are relevant to be included in this comparison in order to better illustrate how different constellation parameters influence the positioning metrics.

5) OptGlobal [6]: this is a Pareto-optimal LEO-PNT constellation taken from our previous work, which was optimized on the global grid seen in Fig. 1.
6) OptAfrica [5]: this Pareto-optimal constellation is another optimized constellation from our previous work, optimized over the Africa grid from Fig. 1.
7) Xona-like [25]: Xona Space Systems' Pulsar constellation is pioneering commercial LEO-based PNT system, belonging to US and designed to complement GNSS with encrypted, high-power navigation signals from low Earth orbits.
8) SouthKoreaConstell [26]: The South Korea Constellation is a LEO-PNT constellations recently proposed in [26] as a part of the future Korean Positioning System (KPS) and designed to enhance the regional GNSS constellation.

It is to be noted that some of the benchmark constellations are not designed as a stand-alone LEO-PNT solution, but rather as augmentation to GNSS. Yet, for fairness reasons, in our comparisons Table II and Figs. 3 to 7 we focus on stand-alone performance metrics described below:

- $\mathcal{C}_{4f}$ and $\mathcal{C}_{1f}$: these values show the percentage of the user tracks in the considered region (Europe, Africa or world) having at least 4 (or 1, respectively), satellites in view. For PNT purposes, the $\mathcal{C}_{4f}$ values are relevant, but $\mathcal{C}_{1f}$ can also be informative for studies related to virtual-satellite positioning, as discussed in Section II.
- The Geometric and Position Dilution of Precisions (GDOP/ PDOP) [28]: these are measuring the 'goodness' of the geometry of the visible satellites; a lower number signals a better geometry.
- EIPR: this is only an informative column about the satellite transmission powers, to illustrate its adjustment according to the carrier frequency.
- The average received power (Rx power) for all visible satellites; the higher, the better. Clearly, indoor scenarios suffer of more path losses than outdoor scenarios and higher frequencies attenuate the signal more than lower carrier frequencies.
- The average carrier-to-noise ratio (C/N_0) taken over all visible satellites. C/N_0 goes hand in hand with the Rx power and it is an indirect measure of how well the acquisition and tracking stages can work; the higher, the better.

While the Table II and bar plots in Figs. 3 and 4 show the average values over the visible satellites, the box-plots in Figs. 5, 6 and 7 are also showing the distribution of the parameters of interest (GDOP, C/N_0, and number of visible satellites N_{SV}). These distributions are a measure of the 'stability' of the positioning solutions: larger spreads with many outliers signal a less stable solution than lower spreads with a low number of outliers.

V. Design Recommendations and Conclusions

One of the main findings in our article is the ability to optimize LEO-PNT constellations for regional uses, e.g., for Europe and polar region as addressed in here, and to achieve very good positioning performance metrics with a much lower constellation size than those not-optimized over the desired region. For example, a constellation with only 66 satellites (OptEurope3) can reach 99.9% four-fold coverage outdoors, similarly with much larger constellations (of more than 200 satellites) and significantly better than similar small-sized constellations (Iridium Next and OptAfrica) which were not optimized for European region. Moreover, good GDOP values (below 5) are achievable with all three newly proposed European constellations, in both indoor and outdoor scenarios and for both considered frequency ranges (UHF & S bands). Another finding is that, by relaxing the conditions on the orbital eccentricity, and allowing a small, but non-zero eccentricity, one can adapt the constellations better to regional coverages.

In terms of comparative performance between the world regions, the positioning metrics most affected by the geographical region are the coverage and the GDOP; the C/N_0 remains pretty stable across various geographical regions. We can also see from the presented results that the most significant trade-off is between the achievable performance and the number of satellites in the constellations. Constellations with more than 200 satellites can easily reach 100% four-fold outdoor coverage, while constellations with less than 100 satellites struggle to reach the perfect 100% four-fold outdoor coverage, although they can still reach more than 99.9% when properly optimized.

Another important design aspect is the stability of the results, as depicted by the box-plots in Figs. 6, 5, and 7. The three proposed constellations (OptEurope1-3) have a stable behaviour compared to the other benchmarks, in particular over the European region where they were optimized for, pointing out towards a promising path towards regional applications based on LEO-PNT. Our findings are also promising in the context of Integrated Communication and Navigation (ICAN) paradigm in the context of LEO. Indeed, over the last few years, a strong international research and industrial push has emerged toward integrating communication and navigation functions within LEO satellite constellations. This trend is driven by advances in satellite technology, the rise of the "NewSpace" concept and clear performance limitations of regional/local PNT and communication systems. ICAN solutions will use shared waveforms, shared spectrum, shared hardware, and common network infrastructure to simultaneously deliver broadband communication, high-precision robust navigation, and possibly sensing, e.g., in future 6G architectures. Our multi-criteria optimization framework is scalable to other criteria in the optimization process, to encompass also the communications and sensing aspects.

As for the limitation of the current study to single-shell optimization, this focus on the single-shell configurations was justified by the complexity of the optimization problem. In general, the complexity of NGSA-III algorithm is in the order

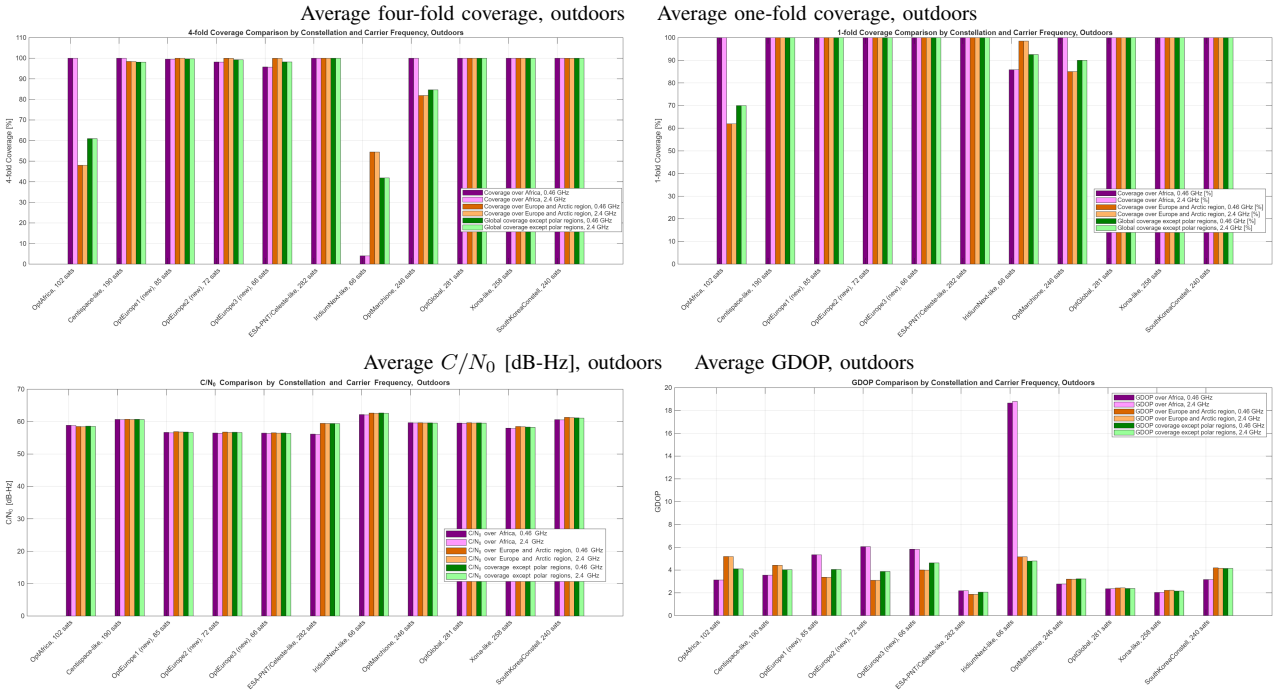

Fig. 3. Outdoor average statistics for 11 constellations - three newly proposed and eight benchmarks. $f_c = 2.4$ GHz and $P_T = -127$ dBm. The bar plots correspond to three grid regions and two carrier frequencies. Same colour with different nuances is used for the same region; pale colours are for 2.4 GHz and strong colours for 0.46 GHz.

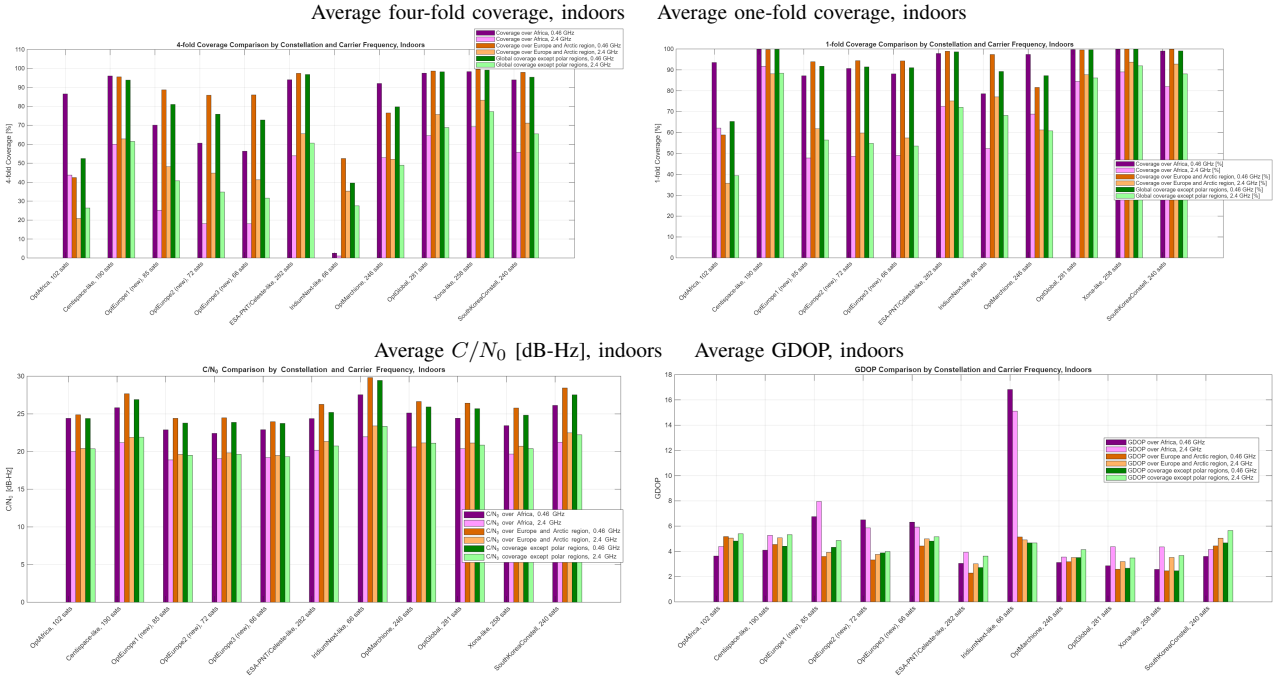

Fig. 4. Indoor average statistics for 11 constellations - three newly proposed and eight benchmarks. $f_c = 0.46$ GHz and $P_T = -155$ dBm. The bar plots correspond to three grid regions and two carrier frequencies. Same colour with different nuances is used for the same region; pale colours are for 2.4 GHz and strong colours for 0.46 GHz.

of O(MN_{pop}^2) [29], with M being the number of optimization parameters (e.g., $M = 6$ in our model and $M = 6N_{shells}$ if the number of shells is also included in the optimization), and N_{pop} is the population size, which is proportional to the size of the optimization space $\mathcal{S}_{\mathbf{x}}$, that depends on the number of the objectives in the optimization metric as well as on the optimization constraints. Thus, the proposed approach can be extended to a multi-shell optimization as well as for an increased number of optimization objectives, but at the expense of a higher computational complexity and time.

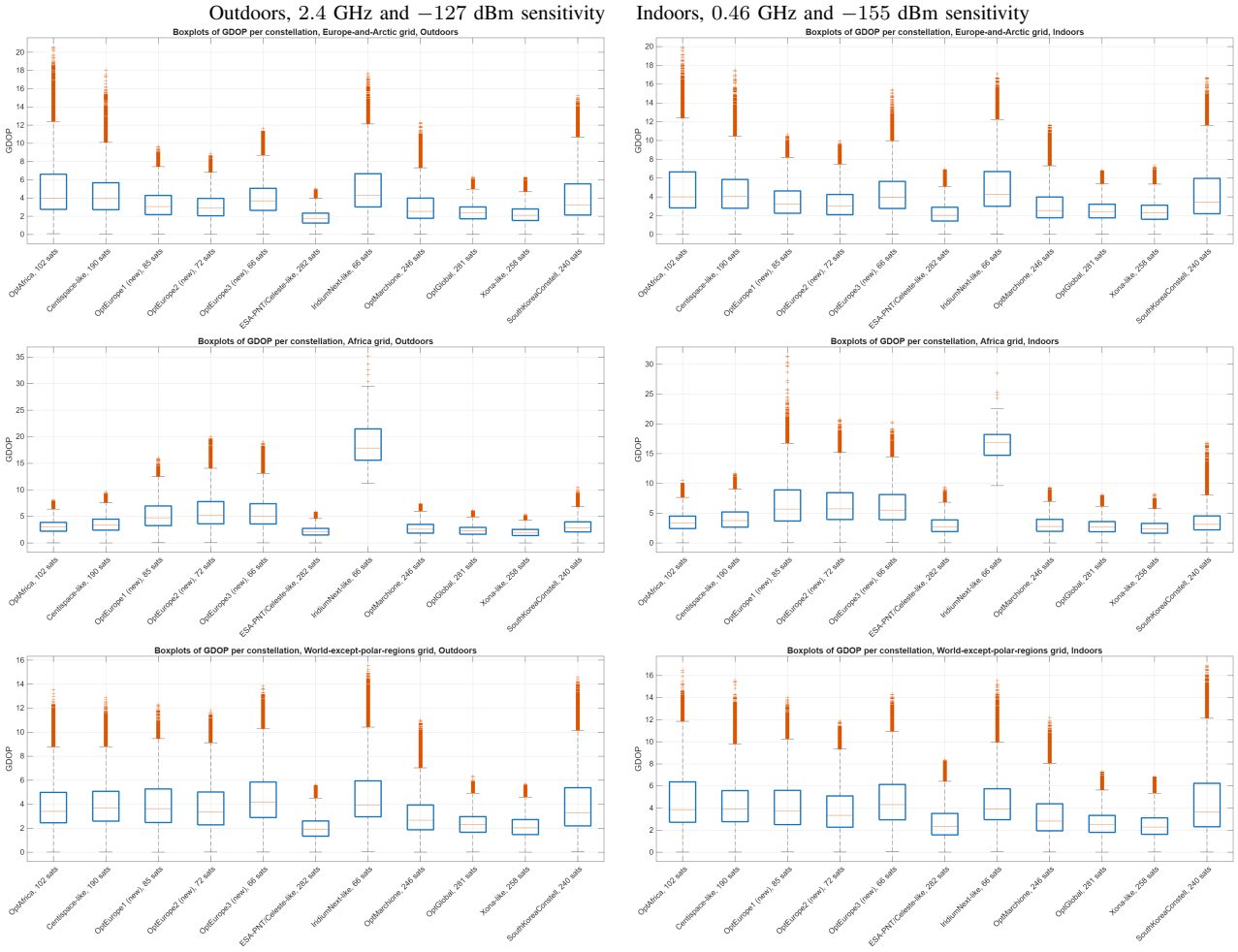

Fig. 5. Box-plot comparisons of achievable $GDOP$ with 11 considered constellations under two carrier frequencies. Upper plots: European region including the Arctic region; middle plots: African region; lower plots: world-wide region except the polar regions. Left-side plots: Outdoors, $f_c = 2.4$ GHz, $P_T = -127$ dBm. Right-side plots: Indoors, $f_c = 0.46$ GHz, $P_T = -155$ dBm.

As final remarks, our study showed that regionally optimized LEO-PNT constellations can deliver performance levels comparable to three-times larger constellations, while requiring significantly fewer satellites, and thus, with reduced costs. By extending our multi-objective optimization framework to Europe and Arctic regions, by incorporating additional optimization metrics, and by adding the orbital eccentricity as an optimization parameter, we showed that single-shell constellations with 66–85 satellites can achieve robust coverage, carrier-to-noise ratios, and dilution of precision under both indoor and outdoor conditions, and at both UHF and S frequency bands. These findings highlight the potential for cost-effective, resilient, and adaptable PNT solutions tailored to regional needs, scalable also to joint communication and navigation optimization targets, and enabling strategic autonomy, disaster response capabilities, and secure alternatives in scenarios where primary systems are compromised. Our findings pave the road towards opening up a wide range of strategic, technological, and societal opportunities such as low-cost positioning solutions optimized for disaster-prone regions, regional autonomy and alternative positioning solutions in case when the main ones are spoofed, as well as facilitating joint inter-regional operations with trusted partners.

ACKNOWLEDGMENT

This work has been supported by the LEDSOL project funded within the LEAP-RE programme by the European Union's Horizon 2020 Research and Innovation Program under Grant Agreement 963530 and the Research Council of Finland (RCF) grant 352364 as well as by the the CHIST-ERA Multi-GIS call 2023, through UEFISCDI, project number ERANET-CHISTERA-IV-ROBOSAT within PNCDI IV and RCF grant 368663 for ROBOSAT project.

REFERENCES

[1] L. Ries, M. C. Limon, F.-C. Grec, M. Anghileri, R. Prieto-Cerdeira, F. Abel, J. Miguez, J. V. Perello-Gisbert, S. D'Addio, R. Ioannidis, A. Ostillio, M. Rapisarda, R. Sarnadas, and P. Testani, "LEO-PNT for augmenting Europe's space-based PNT capabilities," in *2023 IEEE/ION Position, Location and Navigation Symposium*, 2023. doi: 10.1109/PLANS53410.2023.10139999 pp. 329–337.

[2] F. S. Prol and et al., "Position, navigation, and timing (PNT) through low earth orbit (LEO) satellites: A survey on current status, challenges, and opportunities," *IEEE Access*, vol. 10, pp. 83 971–84 002, 6 2022.

[3] "European Space Agency - Celeste, Resilience and robustness for navigation," https://www.esa.int/Applications/Satellite_navigation/Celeste, 2025.

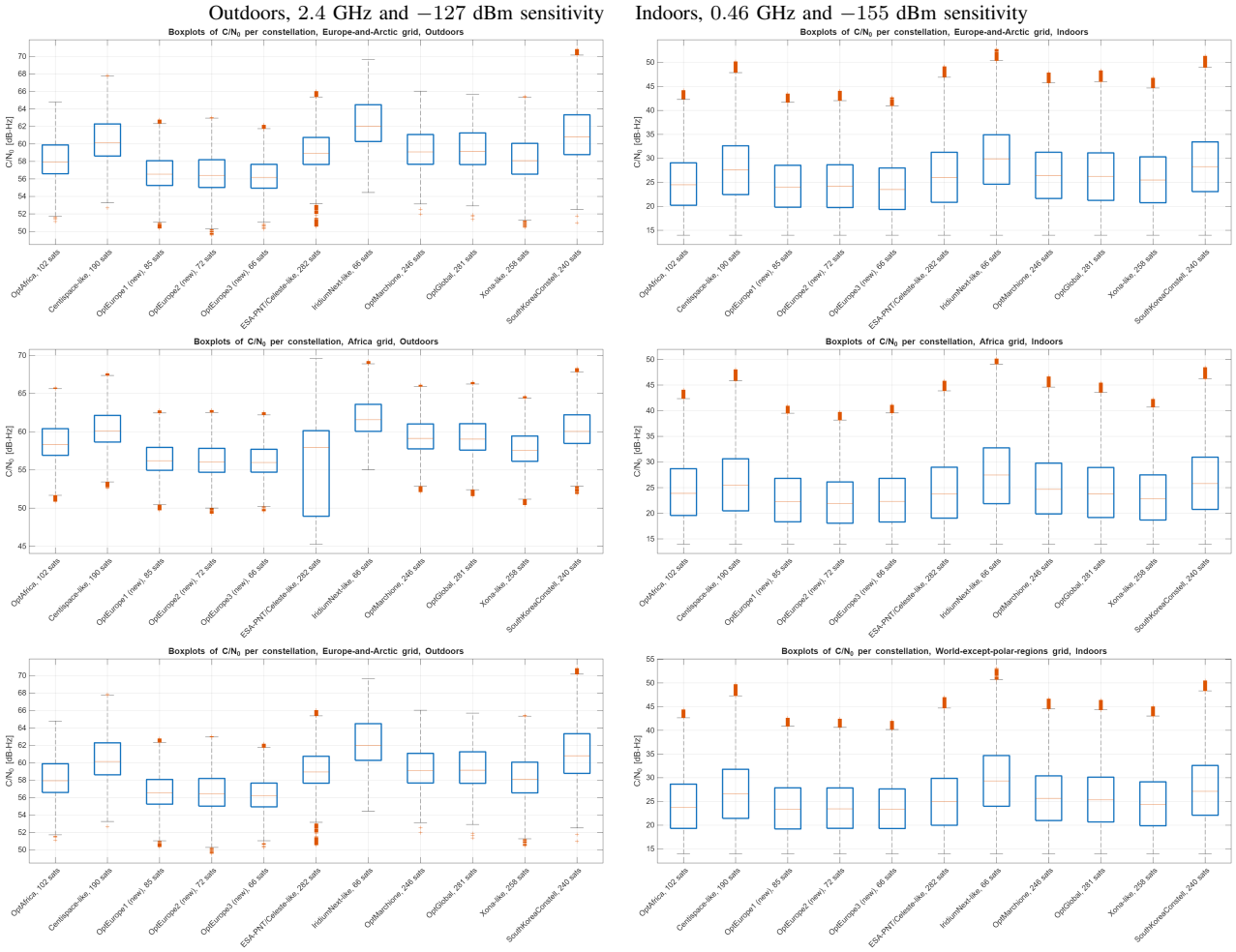

Fig. 6. Box-plot comparisons of achievable C/N_0 with the 11 considered constellations under various indoor and outdoor conditions. Upper plots: European region including Arctic region; middle plots: African region; lower plots: world-wide region except the polar regions. Left-side plots: Outdoors, $f_c = 2.4$ GHz, $P_T = -127$ dBm. Right-side plots: Indoors, $f_c = 0.46$ GHz, $P_T = -155$ dBm.

[4] "European Space Agency - LEO-PNT Pathfinder A," https://www.esa.int/esearch?q=PathFinder-A, 2025.

[5] E. S. Lohan, K. Celikbilek, and O. Cramariuc, "Constellation optimization for Low-Earth-Orbit- based positioning services in African region," in *2025 International Conference on Software, Telecommunications and Computer Networks (SoftCOM)*, 9 2025. doi: 10.23919/SoftCOM66362.2025.11197360 pp. 1–6.

[6] K. Celikbilek, E. S. Lohan, and J. Praks, "Optimization of a LEO-PNT constellation: Design considerations and open challenges," *International Journal of Satellite Communications and Networking*, 2 2025.

[7] W. Xie, G. Huang, W. Fu, S. Du, B. Cui, M. Li, and Y. Tan, "Rapid estimation of undifferenced multi-gnss real-time satellite clock offset using partial observations," *Remote Sensing*, vol. 15, no. 7, 2023.

[8] A. Dyukov, "Mask angle effects on gnss speed validity in multipath and tree foliage environments," *Asian Journal of Applied Sciences*, vol. 4, 4 2022.

[9] T. A. Stansell *et al.*, "Transit, the navy navigation satellite system," *NAVIGATION: Journal of the Institute of Navigation*, vol. 18, no. 1, pp. 93–109, 1971.

[10] R. J. Danchik, "An overview of transit development," *Johns Hopkins APL technical digest*, vol. 19, no. 1, p. 19, 1998.

[11] S. Jaeckel, L. Raschkowski, K. Börner, L. Thiele, F. Burkhardt, and E. Eberlein, "Quadriga - quasi deterministic radio channel generator, user manual and documentation," Fraunhofer Heinrich Hertz Institute, Berlin, Germany, Tech. Rep., 2020. [Online]. Available: https://quadriga-channel-model.de/?download=32621 (Accessed March 26, 2026).

[12] S. Jaeckel, L. Raschkowski, and L. Thieley, "A 5G-NR satellite extension for the QuaDRiGa channel model," in *2022 Joint European Conference on Networks and Communications & 6G Summit*, 2022. doi: 10.1109/EuCNC/6GSummit54941.2022.9815679 pp. 142–147.

[13] "Propagation data required for the design of broadcasting-satellite systems," International Telecommunication Union, Radiocommunication Sector (ITU-R), Tech. Rep. Recommendation ITU-R P.679-3, February 2001, approved in 2001-02. [Online]. Available: https://www.itu.int/dms_pubrec/itu-r/rec/p/R-REC-P.679-3-200102-S!!PDF-E.pdf

[14] P. F. Bronson and B. G. Gladstone, "Schedule and cost estimating analysis for leo satellite constellations," Institute for Defense Analyses, Alexandria, VA, Technical Report NS D-33436, April 2023, approved for public release; distribution is unlimited. [Online]. Available: https://www.ida.org/-/media/feature/publications/s/sc/schedule-and-cost-estimating-analysis-for-leo-satellite-constellations/d-33436.ashx

[15] R. Fitzpatrick, *An Introduction to Celestial Mechanics*. Cambridge: Cambridge University Press, 2012, accessed via ProQuest Ebook Central. [Online]. Available: https://ebookcentral.proquest.com/lib/yourlibrary/detail.action?docID=XXXXXX

[16] M. Li and X. Yao, "What Weights Work for You? Adapting Weights for Any Pareto Front Shape in Decomposition-Based Evolutionary Multiobjective Optimisation," *Evolutionary Computation*, vol. 28, no. 2, pp. 227–253, 06 2020. [Online]. Available: https://doi.org/10.1162/evco_a_00269

[17] K. Çelikbilek, Z. Saleem, R. Morales Ferre, J. Praks, and E. S. Lohan, "Survey on optimization methods for leo-satellite-based networks with applications in future autonomous transportation," *Sensors*, vol. 22, no. 4, 2 2022.

[18] K. Deb and H. Jain, "An evolutionary many-objective optimization algorithm using reference-point-based nondominated sorting approach,

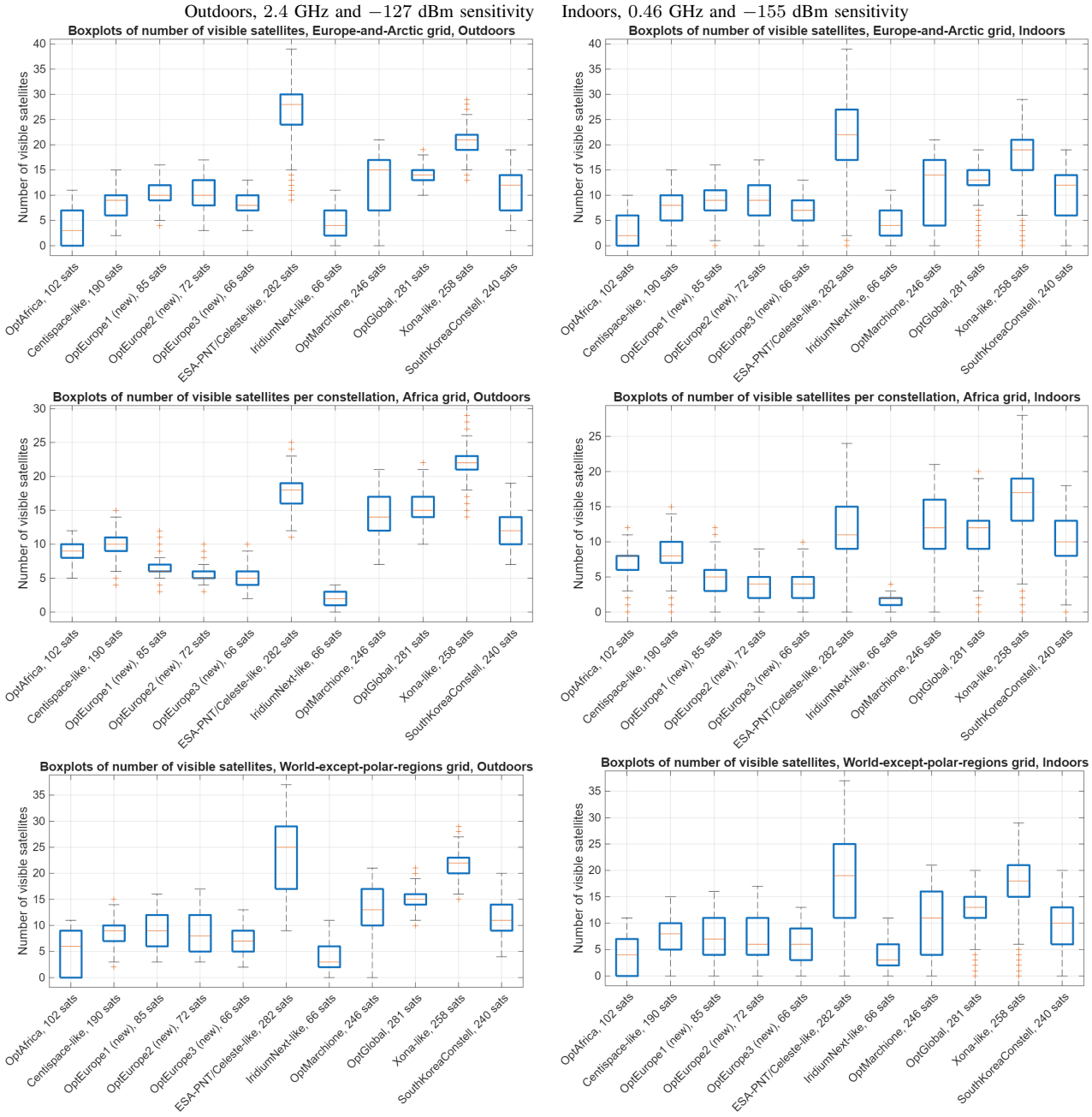

Fig. 7. Box-plot comparisons of the number of visible satellites with the 11 considered constellations under various indoor and outdoor conditions. Upper plots: European region including Arctic region; middle plots: African region; lower plots: world-wide region except the polar regions. Left-side plots: Outdoors, $f_c = 2.4$ GHz, $P_T = -127$ dBm. Right-side plots: Indoors, $f_c = 0.46$ GHz, $P_T = -155$ dBm.

part i: Solving problems with box constraints," *IEEE Transactions on Evolutionary Computation*, vol. 18, no. 4, pp. 577–601, 2014.

[19] H. Jain and K. Deb, "An evolutionary many-objective optimization algorithm using reference-point based nondominated sorting approach, part ii: Handling constraints and extending to an adaptive approach," *IEEE Transactions on Evolutionary Computation*, vol. 18, no. 4, pp. 602–622, 2014.

[20] H. Ishibuchi, Y. Setoguchi, H. Masuda, and Y. Nojima, "Performance of decomposition-based many-objective algorithms strongly depends on pareto front shapes," *IEEE Transactions on Evolutionary Computation*, vol. 21, no. 2, pp. 169–190, 2017.

[21] B. Eissfeller, T. Pany, D. Dötterböck, and R. Förstner, "A comparative study of LEO-PNT systems and concepts," in *Proc. of the ION Pacific PNT Meeting*, ser. PNT 2024. Institute of Navigation, 5 2024. doi: 10.33012/2024.19646. ISSN 2331-6284

[22] H. Ge, B. Li, M. Ge, N. Zang, L. Nie, Y. Shen, and H. Schuh, "Initial assessment of precise point positioning with LEO enhanced global navigation satellite systems (LeGNSS)," *Remote Sensing*, vol. 10, no. 7, Jun. 2018. [Online]. Available: http://dx.doi.org/10.3390/rs10070984

[23] M. Xucheng, "Centispace LEO augmentation navigation system status," Slides at Workshop on Low Earth Orbit Positioning Navigation and Timing Systems, https://www.unoosa.org/documents/pdf/icg/2023/ICG_WG-S_LEO-PNT_Workshop_June_2023/ICG_LEO-PNT_Workshop_2023_01.pdf, 2023.

[24] L. Marchionne, L. M. Gessato, F. Toni, and S. L. Barbera, "Striking a balance: Performance and cost optimization of LEO-PNT constellation for hybrid users using a meta-heuristic approach," in *IEEE 10th Int. Workshop on Metrology for AeroSpace*. IEEE, 2023. doi: 10.1109/MetroAeroSpace57412.2023.10189946

[25] B. Chan, P. Shannon, P. Giordano, R. P. C. amnd Andrés Juez Muñoz, M. Monnerat, S. Kogure, M. Murata, and J. Critchley-Marrows, "State of the Market Report Low Earth

Orbit Positioning Navigation and Timing – 2024 Edition." [Online]. Available: https://frontiersi.com.au/wp-content/uploads/2025/01/FrontierSI-State-of-Market-Report-LEO-PNT-2024-Edition-v1.1.pdf

[26] H.-J. Lee, Y.-J. Song, S. Lee, and J.-H. Won, "Performance analysis of LEO PNT constellations," in *2025 IEEE/ION Position, Location and Navigation Symposium (PLANS)*, 2025. doi: 10.1109/PLANS61210.2025.11028449 pp. 404–409.

[27] "Iridium NEXT engineering statement- appendix 1," https://fcc.report/IBFS/SAT-MOD-20131227-00148/1031348.pdf, 2013, accessed: 2025-05-13.

[28] E. D. Kaplan and C. J. Hegarty, *Understanding GPS, Principles and Applications. 3rd Edition*. Artech House, 2017.

[29] K. Deb, A. Pratap, S. Agarwal, and T. Meyarivan, "A fast and elitist multiobjective genetic algorithm: Nsga-ii," *IEEE Transactions on Evolutionary Computation*, vol. 6, no. 2, pp. 182–197, 4 2002.

Elena Simona Lohan (*Senior Member, IEEE*) is a professor and the leader of TLTPOS research group on Signal processing for wireless positioning at Tampere University and a Visiting Professor at Universitat Autonoma de Barcelona. She is a co-editor of the first book on Galileo satellite system (Springer "Galileo Positioning technology"), and author or co-author in more than 300 international peer-reviewed publications.

Kaan Çelikbilek received his B.Sc. (Tech.) degree in electrical and electronics engineering from Bilkent University in 2018, the M.Sc. (Tech.) degree in robotics and artificial intelligence from Tampere University in 2020, and the PhD (Dr. Tech) degree in wireless communications in 2025, also at Tampere University. His research interests include deep learning, reinforcement learning, multi-objective optimization, satellite communication, GNSS, computer vision, and robotics.

Oana Cramariuc received her Ph.D. in Computational Physics from Tampere University of Technology. She is currently the CEO of Centrul IT pentru Știință și Tehnologie (CITST), a Romanian SME with a strong focus on research and innovation in fields such as ICT and robotics. At CITST, she has contributed to numerous European projects, leveraging her scientific and industrial expertise to foster collaboration between researchers, authorities, and communities.